The Canadian Mineralogist
Vol. 37, pp. 1369-1384 (1999)

THE MINERALOGY OF A UNIQUE BARATOVITE- AND MISERITE-BEARING QUARTZ – ALBITE – AEGIRINE ROCK FROM THE DARA-I-PIOZ COMPLEX, NORTHERN TAJIKISTAN

EKATERINA P. REGUIR AND ANTON R. CHAKHMOURADIAN[§]

Department of Geology, Lakehead University, 955 Oliver Road, Thunder Bay, Ontario P7B 5E1, Canada

MIKHAIL D. EVDOKIMOV

Department of Mineralogy, St. Petersburg State University, 7/9 University Quay, St. Petersburg, 199034, Russia

ABSTRACT

Metasomatic rocks of the Dara-i-Pioz alkaline complex in northern Tajikistan are known to contain a great variety of rare silicates enriched in Li, B, F and incompatible elements. One example is a quartz – albite – aegirine rock from the Upper Dara-i-Pioz intrusion, which is interpreted as a product of metasomatic alteration of an alkaline syenite parent. The bulk of the rock, an assemblage of aegirine–hedenbergite, albite, microcline and fluorapatite, formed during an albitization event. Unusual K–Ca silicates that crystallized during this stage include baratovite $KLi_3Ca_7Ti_2[Si_6O_{18}]_2F_2$, miserite $K_{1.3}(Ca,\mathit{REE})_6[Si_8(O,OH)_{22}](OH,F)_2$ and turkestanite $(K,Pb)_{0.5}(Ca,Na,\mathit{REE},Pb)_2(Th,U,\mathit{REE})[(Si,Al)_8O_{20}]$ (formulae given on the basis of compositional data). Sr-bearing calcite postdates the albitization assemblage, and may be a manifestation of a distinct metasomatic event (carbonatization). Conspicuous strain-induced features exhibited by the clinopyroxene, quartz, baratovite, miserite, microcline and calcite indicate that the rock underwent deformation during the late stages of crystallization. Deformation-induced fracturing of the rock facilitated circulation of a relatively low-temperature fluid enriched in B, F, Ti and incompatible elements. The fluid precipitated datolite, fluorite, quartz, and a rich diversity of rare minerals containing *REE*, Ba, Zr, Sn, Hf and Nb. The *REE* are concentrated predominantly in the borosilicates tadzhikite $Ca_{3.2–3.8}\mathit{LREE}_{1.0–1.8}Y_{0.1–0.9}(Ti,Fe,Al)_{1.0}[B_4Si_4O_{20.3}(OH)_{1.7}](OH)_2$ and stillwellite-(Ce) $\mathit{LREE}[BSiO_5]$. The new analytical data confirm the existence of two distinct mineral species, "tadzhikite-(Y)" and "tadzhikite-(Ce)". The high-field-strength elements and Ti are concentrated in titanite (≤8.1 wt.% SnO_2, 2.3 wt.% ZrO_2 and 1.7 wt.% Nb_2O_5), bazirite (≤2.9 wt.% SnO_2, 2.1 wt.% HfO_2) and zircon (≤3.2 wt.% HfO_2). The B–F-enriched fluid may have been derived from alkaline pegmatites that cut the metasomatic suite and contain a similar assemblage of rare minerals.

Keywords: aegirine, baratovite, bazirite, miserite, stillwellite, tadzhikite, titanite, metasomatic assemblage, alkaline complex, Dara-i-Pioz, Tajikistan.

SOMMAIRE

Les roches métasomatiques du complexe alcalin de Dara-i-Pioz, dans le nord du Tajikistan, sont connues pour la grande diversité de silicates rares enrichis en Li, B, F et éléments incompatibles. Par exemple, la roche à quartz – albite – aegyrine provenant de la partie supérieure du massif intrusif de Dara-i-Pioz serait le produit d'une métasomatose d'une syénite alcaline. En grande partie, cette unité, constituée d'un assemblage d'aegyrine–hédenbergite, albite, microcline et fluorapatite, se serait formée au cours d'un épisode d'albitisation. Parmi les silicates rares à K–Ca de ce stade, on trouve baratovite $KLi_3Ca_7Ti_2\,[Si_6O_{18}]_2\,F_2$, miserite $K_{1.3}(Ca,\mathit{TR})_6\,[Si_8(O,OH)_{22}]\,(OH,F)_2$, et turkestanite $(K,Pb)_{0.5}\,(Ca,Na,\mathit{TR},Pb)_2(Th,U,\mathit{TR})\,[(Si,Al)_8O_{20}]$ (les formules sont illustratives des données obtenues). Le développement d'une calcite strontifère a suivi l'épisode d'albitisation, et pourrait témoigner d'un épisode métasomatique distinct (carbonatisation). Clinopyroxène, quartz, baratovite, miserite, microcline et calcite font preuve de déformation tardive. Les fractures qui en ont résulté ont facilité la circulation d'une phase fluide enrichie en B, F, Ti et éléments incompatibles à température relativement faible. Datolite, fluorite, quartz, et une riche diversité de minéraux rares contenant les terres rares (*TR*), Ba, Zr, Sn, Hf et Nb se sont formés à ce stade. Les terres rares sont concentrées surtout dans les borosilicates tadzhikite $Ca_{3.2–3.8}\mathit{TRL}_{1.0–1.8}Y_{0.1–0.9}(Ti,Fe,Al)_{1.0}\,[B_4Si_4O_{20.3}\,(OH)_{1.7}]\,(OH)_2$ et stillwellite-(Ce) $\mathit{TRL}\,[BSiO_5]$ (*TRL*: terres rares légères). Les données analytiques nouvelles confirment l'existance de deux espèces distinctes de tadzhikite, à dominance d'yttrium et de cérium, respectivement. Les éléments à potentiel ionique élevé et le titane sont concentrés dans la titanite (≤8.1% SnO_2, 2.3% ZrO_2 et 1.7% Nb_2O_5, en poids), la bazirite (≤2.9% SnO_2, 2.1% HfO_2) et le zircon (≤3.2% HfO_2). La phase fluide enrichie en B et F aurait possiblement été dérivée d'une suite de pegmatites alcalines qui recoupent les roches métasomatiques et qui contiennent aussi un assemblage semblable de minéraux rares.

(Traduit par la Rédaction)

Mots-clés: aegyrine, baratovite, bazirite, miserite, stillwellite, tadzhikite, titanite, assemblage métasomatique, complexe alcalin, Dara-i-Pioz, Tajikistan.

[§] *E-mail address*: achakhmo@gale.lakeheadu.ca

INTRODUCTION

During the last three decades, the Dara-i-Pioz (Dara-Pioz, Darai Piyez) alkaline complex in northern Tajikistan has become very well known for minerals enriched in rare-earth elements (*REE*), Zr, Li, Be, B and Ba, including tadzhikite, baratovite, darapiozite, sogdianite, zektzerite and tienshanite (Belakowski 1991). As is commonly the case, there has been no systematic study of rock-forming minerals from Dara-i-Pioz, and only a few researchers have attempted to consider the unique mineralogy of this complex in a context of geological processes (*e.g.*, Grew *et al.* 1993). Important phases, albeit "ordinary" in terms of chemistry, such as aegirine, apatite and titanite, have been generally neglected.

In this work, we present new data on the petrography and mineralogy of a quartz – albite – aegirine rock from Dara-i-Pioz. We also discuss the occurrence and composition of accessory Ti-, Zr- and *REE*-bearing minerals in this rock, as well as their interrelationships, and some implications of these data for the genesis and evolution of the host rock. The samples used in this study were kindly provided by V.D. Dusmatov, the pioneer in geological exploration of this unusual alkaline complex.

OCCURRENCE

The Dara-i-Pioz alkaline complex is situated in the Garm region of northern Tajikistan (39°25' N, 70°44' E). The complex consists of two distinct intrusions (Middle and Upper) covering a total area of approximately 25 km^2. Each of the intrusions comprises older granites and alkali granites surrounding a core of younger quartz syenite and alkali syenite (Dusmatov *et al.* 1973). These igneous rocks are of Jurassic age (150–190 Ma), and intrude Middle to Upper Paleozoic sedimentary rocks, including shales, sandstones and limestones. The intrusive series and the surrounding sedimentary rocks host mineralogically complex pegmatites and rocks inferred to be of metasomatic origin (Dusmatov *et al.* 1973, Belakowski 1991). The latter are believed to result from two major events, albitization and carbonatization (Dusmatov *et al.* 1973). The metasomatic units, up to 100 m in thickness, are developed predominantly within the alkaline intrusions, and probably confined to fault zones (Belakowski 1991). Metasomatic rocks have diffuse contacts with the wallrock intrusive series, and are cross-cut by alkaline pegmatites of Group 2 (Grew *et al.* 1993). This type of pegmatite contains the greatest diversity of rare minerals enriched in *REE*, Zr, Li, Be, B and Ba (Belakowski 1991).

The metasomatic rock examined in the present study originates from the Upper intrusion, where it occurs in the aegirine–quartz syenites. The rock is modally dominated by albite, quartz, clinopyroxene and microcline, but also contains appreciable amounts of calcite and datolite. Several rare minerals enriched in Ti, Zr, Li, *REE* and B are present here as accessory constituents (Table 1). Replacement and resorption textures, irregular patterns of zonation and other features indicative of disequilibrium during crystallization are common. The observed mineralogical and textural complexity suggests that this rock represents an overprint of two or three distinct hydrothermal–metasomatic events. Four

TABLE 1. RARE MINERALS FROM QUARTZ-ALBITE-AEGIRINE ROCK, DARA-I-PIOZ COMPLEX

MINERAL	FORMULAE ACCORDING TO FLEISCHER (1987)	STRUCTURAL FORMULAE	EMPIRICAL FORMULAE (THIS WORK)
BARATOVITE	$KCa_7(Ti,Zr)_2Li_3Si_{12}O_{36}F_2$	$KLi_3Ca_7Ti_2[Si_6O_{18}]_2F_2$ (MENCHETTI & SABELLI 1979)	$KLi_3Ca_7Ti_2[Si_6O_{18}]_2F_2$
BAZIRITE	$BaZrSi_3O_9$		$(Ba,Ca,Na)_{1.1}(Zr,Sn)[Si_3O_9]$
MISERITE	$K(Ca,Ce)_4\ Si_5O_{13}(OH)_3$	$KCa_5\square[Si_2O_7][Si_6O_{15}](OH)F$ (SCOTT 1976)	$K_{1.3}(Ca,REE)_6\ [Si_8(O,OH)_{22}](OH,F)_2$
STILLWELLITE	$(Ce,La,Ca)BSiO_5$	*LREE*$[BSiO_5]$ (BURNS *ET AL.* 1993)	*LREE*$[BSiO_5]$
TADZHIKITE	$Ca_3\ (Ce,Y)_2(Ti,Al,Fe^{3+})B_4Si_4O_{22}$	$Ca_2\ (Ca,Y)_2(Ti^{4+},Fe^{3+})(R^{3+}\square)_2$ $[B_4Si_4O_{16}(O,OH)_6](OH)_2$ (HAWTHORNE *ET AL.* 1998)	$Ca_{3.2\text{-}3.8}LREE_{1.0\text{-}1.8}Y_{0.1\text{-}0.9}(Ti,Fe^{3+},Al)_{1.0}$ $[B_4Si_4(O,OH)_{22}](OH)_2$
TURKESTANITE		$Th(Ca,Na)_2(K_{1-x}\square_x)[Si_8O_{20}]\cdot nH_2O$ (PAUTOV *ET AL.* 1997)	$(K,Pb)_{0.5}(Ca,Na,REE,Pb)_2$ $(Th,U,REE)[(Si,Al)_8O_{20}]$

samples of the rock examined in the present study exhibit some variation in modal composition and relative abundances of rare phases. Following the common practice of naming metasomatic assemblages according to their modal composition, we use the purely descriptive name "quartz – albite – aegirine rock" to characterize our samples. As neither albite nor clinopyroxene account for more than 50 vol.% of the rock in any of the samples, the terms aegirinite and albitite should not be used here.

The quartz – albite – aegirine rock has an inequigranular texture, and sugary or "micaceous" appearance owing to the presence of fine-grained albite or platy baratovite, respectively. The color index and macroscopic color of the rock vary dramatically on a small scale, and largely depend on the relative proportion of greenish black clinopyroxene, pink miserite, and white patches of albite, quartz and baratovite. Fragmentation, fracturing and bending of mineral grains, coarse twinning, curved cleavage and undulatory extinction observed in most rock-forming minerals suggest that the rock was formed in the presence of stress, possibly in an active fault-zone.

PETROGRAPHY AND MINERAL CHEMISTRY

The minerals described in the present work were identified using optical microscopy, X-ray powder diffractometry and X-ray energy-dispersion spectrometry (EDS). All mineral compositions were determined using a Hitachi 570 scanning electron microscope equipped with a LINK ISIS analytical system incorporating a Super ATW Light Element Detector. Raw EDS spectra were acquired for 100–200 seconds (live time) with an accelerating voltage of 20 kV and a beam current of 0.86 nA. The spectra were processed with the LINK ISIS SEMQUANT software, with full ZAF corrections applied. The lines (and standards) used were Ba*L* (benitoite), Al*K* (corundum), P*K* and F*K*α (fluorapatite), Fe*K* and Ti*K* (ilmenite), Na*K*α (jadeite), La*L*, Ce*L*, Pr*L*, Nd*L* and Nb*L* (loparite), Mn*K* (manganoan fayalite), K*K* (orthoclase), Mg*K* (periclase), Ca*K* and Si*K* (wollastonite), Sr*L* (synthetic $SrTiO_3$), Y*L* (synthetic YF_3), Eu*L* (synthetic EuF_3), Gd*L*, Hf*M*, Pb*M*, Sm*L*, Sn*L*, Ta*M*, Th*M*, Zr*L* and U*M* (pure metals). A multi-element standard for the light *REE* (loparite) was used, as experience has shown that this gives more accurate data than single-*REE* standards when using EDS spectrum-stripping techniques. However, peak profiles used for the analytical X-ray lines were obtained on single *REE* fluoride or metallic standards.

Clinopyroxene is a principal constitutent in the samples examined, and occurs as coarse (~1 cm) prismatic crystals set in a finer-grained matrix of albite, quartz and miserite. Locally, clinopyroxene comprises up to 40–45 vol.% of the rock. The crystals of clinopyroxene are pleochroic from yellow to bright green, and commonly show undulatory extinction and twinning in thin section. The prisms commonly enclose anhedral microcline, euhedral crystals of albite, titanite and miserite, and anhedral fragments of clinopyroxene not in optical continuity with the host. These fragments have slightly different composition (see below), and may represent relics of an earlier generation of clinopyroxene. Most of the prismatic crystals have an embayed margin at the contact with albite, but show no evidence of resorption where rimmed by quartz or microcline. Fractures in clinopyroxene are typically filled with quartz, calcite or fluorite.

Clinopyroxene from the quartz – albite – aegirine rock exhibits a noticeable variation in composition (Table 2, Fig. 1). All clinopyroxene compositions are depleted in Ti and Al, and somewhat enriched in Mn. The clinopyroxene varies from hedenbergite to aegirine-augite at essentially constant contents of other end-members, *i.e.*, $CaMgSi_2O_6$ (13–19 mol.%) and $CaMnSi_2O_6$ (2–4 mol.%). The fragments of early clinopyroxene are enriched in Mg relative to the host prismatic crystals (Fig. 1). As most compositions show a preponderance of the aegirine component over hedenbergite, we simply refer to both varieties of clinopyroxene as aegirine. In the diagram $NaFe^{3+}Si_2O_6$ – $CaFe^{2+}Si_2O_6$ – $CaMgSi_2O_6$, the compositions from Dara-i-Pioz plot near the evolutionary trend for the clinopyroxenes from nepheline syenites of Chinduzi, Malawi (Woolley & Platt 1986). The alternative, high-Mg trend is exhibited by clinopyroxenes from the Lovozero intrusion in Russia and some other alkaline complexes (Fig. 1 and references therein).

The quartz – albite – aegirine rock contains two feldspars, *albite* (15–20 vol.% of the rock) and *microcline* (<5%). Albite forms platy, polysynthetically twinned

TABLE 2. REPRESENTATIVE COMPOSITIONS OF AEGIRINE FROM THE DARA-I-PIOZ COMPLEX

	1	2	3	4	5	6
Na_2O	4.68	5.31	5.25	6.63	6.72	5.25
CaO	15.36	14.42	13.84	11.90	11.30	14.45
MgO	3.06	3.02	2.17	2.26	2.33	2.74
MnO	0.68	0.82	0.97	1.18	0.90	0.91
FeO*	13.86	10.91	12.31	9.23	8.87	12.66
Fe_2O_3*	11.94	12.90	13.72	17.06	17.46	13.36
Al_2O_3	0.16	0.22	0.09	0.16	0.15	0.10
TiO_2	0.24	0.38	0.20	0.25	0.12	0.24
SiO_2	51.16	50.37	49.75	50.69	49.73	51.11
Total	101.14	98.35	98.30	99.36	97.58	100.82
Structural formulae calculated on the basis of 6 atoms of oxygen						
Na	0.353	0.409	0.408	0.506	0.522	0.397
Ca	0.641	0.614	0.595	0.502	0.485	0.604
Mg	0.178	0.179	0.130	0.133	0.139	0.159
Mn	0.022	0.028	0.033	0.039	0.031	0.030
Fe^{2+}	0.451	0.374	0.427	0.317	0.297	0.413
Fe^{3+}	0.350	0.374	0.400	0.493	0.526	0.392
Al	0.007	0.010	0.004	0.007	0.007	0.005
Ti	0.007	0.011	0.006	0.007	0.004	0.007
Si	1.991	2.001	1.996	1.996	1.991	1.993

(1-2) relict aegirine; (3-6) prismatic aegirine.

*FeO and Fe_2O_3 calculated from stoichiometry.

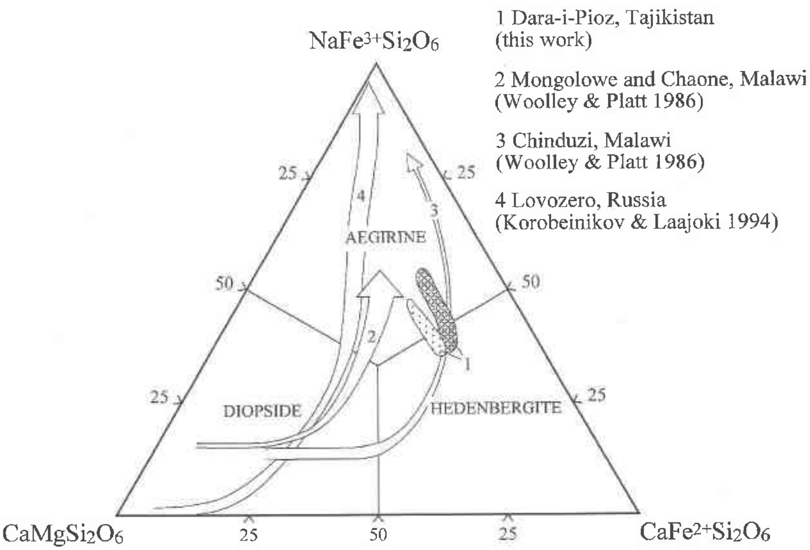

FIG. 1. Compositional variation of clinopyroxene from Dara-i-Pioz and other alkaline intrusive suites. Dotted area corresponds to the compositions of relict clinopyroxene, and cross-hatched area, to those of prismatic clinopyroxene.

crystals smaller than 1 mm in length. Some crystals are enclosed by the prisms of aegirine. In the groundmass, platy crystals of albite associated with elongate prisms of miserite commonly show a weak preferred orientation oblique with respect to aegirine. Microcline occurs as inclusions in aegirine and as equant anhedral grains up to 4 mm in size. The anhedral grains poikilitically enclose smaller crystals of miserite, fluorapatite and, rarely, albite. Both varieties of microcline invariably show a cross-hatched pattern of extinction, but in the large poikilitic grains, twinned domains tend to be concentrated at the margin. Our samples show no evidence of late-stage replacement of microcline by albite, indicating that these two minerals crystallized nearly simultaneously, and in equilibrium with each other. Chemically, both feldspars are close to the corresponding end-member compositions. The two varieties of microcline cannot be distinguished on the basis of their composition, as both contain low levels of Na and Fe (≤0.8 wt.% Na_2O and ≤0.5 wt.% Fe_2O_3), and are characteristically devoid of Ba.

Quartz, the latest rock-forming mineral, succeeded both feldspars, aegirine, baratovite, miserite and fluorapatite. Quartz occurs as anhedral grains in the groundmass and as fracture fillings in the earlier-crystallized phases. The anhedral grains have serrated margins, and invariably show strong undulatory extinction. Margins of most comparatively large grains (1–2 mm) are decorated with smaller (<0.2 mm) rounded grains of quartz showing relatively uniform extinction (Fig. 2a). Such a texture is indicative of syndeformational growth of the smaller quartz grains, also termed subgrain-rotation recrystallization with grain diminution (Hickey & Bell 1996).

Other minerals whose content in the quartz – albite – aegirine rock may locally reach several percent in volume include baratovite, fluorapatite and miserite. These phases were formed relatively early in the crystallization history; baratovite precipitated nearly simultaneously with aegirine, and was followed by miserite and fluorapatite. *Baratovite* forms large (1–8 mm) platy crystals with a distinct pearly luster and a basal cleavage. In thin section, the mineral is characterized by the cleavage, low birefringence, anomalous interference-colors, and typical lengthwise twinning (Figs. 2b, c). The crystals of baratovite are commonly bent, and show undulatory extinction. Some crystals are fractured and host fluorapatite, quartz or albite in the fractures (Fig. 2b).

Baratovite was first described by Dusmatov *et al.* (1975) in quartz – albite – aegirine rocks, and, on the basis of a wet-chemical analysis, given the empirical formula $KLi_2Ca_8Ti_2Si_{12}O_{37}F$. The crystal structure of baratovite was determined by Sandomirskii *et al.* (1976) and, subsequently, by Menchetti & Sabelli (1979). In both cases, the authors proposed a new structural formula, $KLi_3Ca_7Ti_2[Si_6O_{18}]_2F_2$. The only other known occurrence of baratovite is aegirine syenite at Iwagi Islet, Japan, where this mineral was first described under the name "katayamalite" (Murakami *et al.* 1983). The composition of baratovite from Iwagi Islet determined by electron microprobe approaches the formula derived

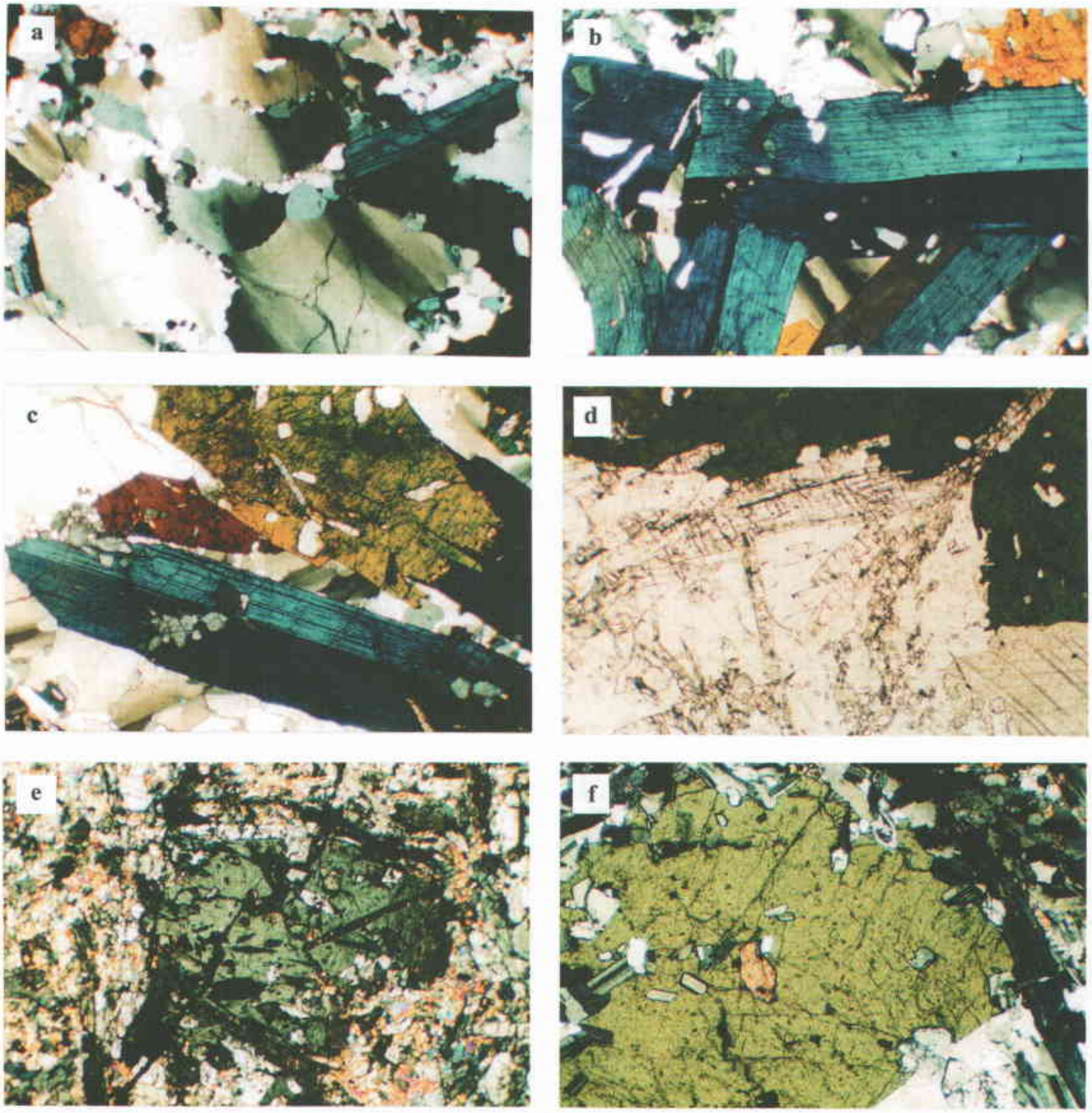

FIG. 2. Mineralogical and textural features of the quartz – albite – aegirine rock, Dara-i-Pioz complex. All photomicrographs except (d) were taken in crossed polars; (d) was taken in plane-polarized light. Width of the field of view in (a)–(c) is 6 mm. (a) Groundmass composed of large grains of quartz with serrated margins and undulatory extinction, and smaller roundish grains. (b) Intergrowth of bent and fractured crystals of baratovite (indigo blue) in a quartz – albite groundmass. (c) Crystals of fluorapatite (grey) in fractures within twinned baratovite; red and green grains are aegirine. (d) Miserite (acicular crystals with high relief and transversal cleavage) enclosed in microcline. Green crystals are aegirine, and cross-hatched grain in the corner is Sr-enriched calcite. Width of the field of view is 4.2 mm. (e) Poikilitic crystal of turkestanite (greenish grey) in a miserite – datolite – quartz groundmass. Most acicular inclusions in turkestanite are miserite. Width of the field of view is 3.7 mm. (f) Inclusions of albite and relict titanite (golden yellow) in aegirine (green). Width of the field of view is 2.7 mm.

from the structural studies, and is poorer in Ca and richer in Li than the type material from Dara-i-Pioz (Dusmatov *et al.* 1975). To resolve this discrepancy in analytical data, we carried out about thirty new analyses of baratovite using EDS. Li contents were calculated from stoichiometry assuming that the F sites coordinating the Ca polyhedra in the structure contain only monovalent anions, but no oxygen atoms (Menchetti & Sabelli 1979). The new analytical data and those from the previous studies are compared in Table 3. Our results

TABLE 3. REPRESENTATIVE COMPOSITIONS OF BARATOVITE

	1	2	3	4
K_2O	2.96	2.87	2.96	2.89
Na_2O	0.43	0.30	0.70	0.22
Li_2O	3.17*	3.54*	2.05	3.25
CaO	27.71	27.61	30.36	28.25
MnO	0.15	0.10	0.12	0.22
TiO_2	11.14	10.71	9.55	10.99
ZrO_2	0.85	0.80	2.28	n.d
Fe_2O_3**	0.30	0.43	0.50	0.29
Nb_2O_5	n.d	n.d	0.72	n.d
SiO_2	52.12	51.98	50.46	52.31
Total	98.83	98.34	99.70†	98.42‡
Structural formulae calculated to 12 atoms of Si				
K	0.869	0.845	0.90	0.85
Na	0.192	0.134	0.28	0.10
Li	2.940*	3.285*	1.96	3.00
Ca	6.843	6.837	7.75	6.94
Mn	0.029	0.020	0.02	0.04
Ti	1.929	1.859	1.71	1.90
Zr	0.095	0.090	0.26	-
Fe**	0.052	0.075	0.09	0.05
Nb	-	-	0.08	-
Si	12.000	12.000	12.00	12.00

(1-2) Dara-i-Pioz, Tajikistan (this work); (3) Dara-I-Pioz (Dusmatov *et al.* 1975); (4) Iwagi Islet, Japan (Murakami *et al.* 1983). *Li_2O calculated from stoichiometry. **Total Fe given as Fe_2O_3. † Total also includes 1.05 wt.% F and -0.44 wt.% $O{\equiv}F_2$. ‡ Total also includes 0.34 wt.% F, 1.21 wt.% H_2O and -0.14 wt.% $O{\equiv}F_2$. n.d = not detected.

TABLE 4. REPRESENTATIVE COMPOSITIONS OF FLUORAPATITE FROM THE DARA-I-PIOZ COMPLEX

Wt.%	1	2	3	4	5
Na_2O	n.d	0.12	0.02	0.20	0.21
CaO	54.83	54.71	54.32	52.29	53.84
SrO	0.75	0.43	1.00	1.21	1.24
La_2O_3	0.10	0.40	0.40	0.54	0.44
Ce_2O_3	0.24	0.35	0.63	1.26	0.80
Nd_2O_3	n.d	n.d	0.09	0.38	0.41
SiO_2	0.01	n.d	n.d	0.64	0.59
P_2O_5	41.74	41.96	42.01	40.05	41.43
F	2.32	2.10	2.89	1.83	3.15
$-O{\equiv}F_2$	0.98	0.88	1.22	0.77	1.33
Total	99.01	99.19	100.14	97.63	100.78
Structural formulae calculated to a total of 8 cations					
Na	-	0.020	0.003	0.034	0.034
Ca	4.965	4.941	4.912	4.848	4.854
Sr	0.037	0.021	0.049	0.061	0.060
La	0.003	0.012	0.012	0.017	0.014
Ce	0.007	0.011	0.019	0.040	0.025
Nd	-	-	0.003	0.012	0.012
Si	0.001	-	-	0.055	0.050
P	2.987	2.995	3.002	2.934	2.951
F	0.620	0.560	0.771	0.501	0.838

(1) and (2) core and rim of a weakly zoned crystal; (3) core and (4-5) rim of a zoned crystal. n.d = not detected. S and Cl were sought, but not found.

are in good agreement with the structural formula suggested by Sandomirskii *et al.* (1976), and almost identical to the microprobe data for "katayamalite" obtained by Murakami *et al.* (1983).

Fluorapatite forms stubby prismatic crystals usually smaller than 0.2 mm in size. They are embedded in albite, microcline and quartz, or confined to fractures within baratovite and other earlier-crystallized minerals (Fig. 2c). In back-scattered electron images (BSE), the crystals show a complex zoning with a thin lighter rim, an irregularly shaped darker core, and a few ill-defined intermediate zones with varying average atomic number. Relative to the core, the rim is invariably enriched in light *REE* (Table 4). For some grains, this zonation is visible in thin section, as the rim has a slightly higher birefringence than the core. The two major mechanisms of substitution responsible for incorporation of *REE* in fluorapatite are $Ca^{2+} + P^{5+} \Leftrightarrow REE^{3+} + Si^{4+}$ and $2Ca^{2+} \Leftrightarrow Na^{+} + REE^{3+}$. Fluorapatite from Dara-i-Pioz has not been previously studied, but alkaline rocks from other occurrences are known to contain apatite-group minerals with significant levels of Sr and *REE* (Pekov *et al.* 1995, Chakhmouradian & Mitchell 1999). Fluorapatite from agpaitic associations typically contains higher Na contents than the material from Dara-i-Pioz (≤0.2 wt.% Na_2O), *i.e.*, it is enriched in the belovite component. Belovite-(Ce), $Na(Ce,La)Sr_3[PO_4]_3F$, is a characteristic accessory constituent of hyperagpaitic pegmatites in nepheline syenite complexes (Pekov *et al.* 1995).

Miserite occurs as acicular crystals of pink color associated with fine-grained albite and fluorapatite. Discrete needles and radiating intergrowths of miserite are commonly enclosed in microcline, quartz and turkestanite. Some needles are bent or attenuated between larger crystals of aegirine (Fig. 2d). Miserite is colorless in thin section, and can be distinguished by its high positive relief, lengthwise cleavage, low birefringence and a bluish anomalous interference-color. In BSE images, this mineral is relatively homogeneous, but locally, along fractures, has a slightly lower atomic number owing to depletion in *REE* (*cf.* anal. 3 and 4 in Table 5). Structural formulae of miserite were recalculated on the basis of eight Si atoms per formula unit, as the proportion of large cations per unit cell is variable, and the quadruple composite "tunnels" of silicate tetrahedra are the only rigid element of the structure (Scott 1976). All analytical data obtained in the present study, including the relatively *REE*-depleted compositions, are consistent with the empirical formula $K_{1.3}(Ca,REE)_6[Si_8(O,OH)_{22}](OH,F)_2$. The ideally vacant *Z* site is partially occupied by potassium atoms (*ca.* 30%), and the six-coordinated *X* site is nearly completely occupied by *REE* + Y and the excess of Ca over 5 *apfu*, atoms per formula unit (*cf.* the structural data of Scott 1976).

TABLE 5. REPRESENTATIVE COMPOSITIONS OF MISERITE FROM THE DARA-I-PIOZ COMPLEX

Wt.%	1	2	3	4
K_2O	6.03	6.45	6.59	6.50
Na_2O	0.07	n.d	0.06	n.d
CaO	31.69	32.36	32.66	32.87
MgO	0.07	n.d	0.08	0.17
MnO	0.20	0.21	0.24	0.24
FeO	n.d	0.10	0.32	0.26
Y_2O_3	4.36	1.49	2.11	0.98
La_2O_3	n.d	0.45	0.09	0.27
Ce_2O_3	0.44	1.71	1.06	1.20
Pr_2O_3	n.d	n.d	0.66	0.09
Nd_2O_3	0.65	1.00	1.36	1.07
Eu_2O_3	n.d	0.20	n.d	0.38
Gd_2O_3	n.d	0.13	n.d	0.46
Sm_2O_3	n.d	0.05	n.d	0.26
TiO_2	n.d	0.11	0.16	0.28
SiO_2	49.46	49.60	50.61	50.66
Al_2O_3	n.d	n.d	0.05	0.11
Total	92.97	93.86	96.05	95.80
Structural formulae calculated on the basis of Si + Al = 8				
K	1.244	1.327	1.327	1.306
Na	0.022	-	0.018	-
Ca	5.492	5.593	5.525	5.548
Mg	0.017	-	0.019	0.040
Mn	0.027	0.029	0.032	0.032
Fe^{2+}	-	0.013	0.042	0.034
Y	0.375	0.128	0.177	0.082
La	-	0.027	0.005	0.016
Ce	0.026	0.101	0.061	0.069
Pr	-	-	0.038	0.005
Nd	0.038	0.058	0.077	0.060
Eu	-	0.011	-	0.020
Gd	-	0.007	-	0.024
Sm	-	0.003	-	0.014
Ti	-	0.013	0.009	0.033
Si	8.000	8.000	7.991	7.980
Al	-	-	0.009	0.020

n.d = not detected.

TABLE 6. REPRESENTATIVE COMPOSITIONS OF TURKESTANITE FROM THE DARA-I-PIOZ COMPLEX

	1	2		1	2
	Wt.%			Structural formulae to 20 atoms of oxygen	
Na_2O	0.96	1.11	Na	0.295	0.344
K_2O	2.22	2.07	K	0.449	0.422
CaO	7.91	8.16	Ca	1.345	1.397
PbO	5.09	5.11	Pb	0.217	0.220
MgO	0.14	0.04	Mg	0.033	0.010
Al_2O_3	0.92	0.64	Al	0.172	0.121
Y_2O_3	0.17	0.33	Y	0.014	0.028
La_2O_3	1.09	0.74	La	0.064	0.044
Ce_2O_3	2.00	1.82	Ce	0.116	0.106
Nd_2O_3	0.56	0.95	Nd	0.032	0.054
ThO_2	22.00	21.38	Th	0.794	0.777
UO_2	5.91	7.42	U	0.108	0.136
SiO_2	49.26	48.93	Si	7.816	7.817
Total	98.23	98.70			

Miserite occurs in a variety of alkaline igneous and metasomatic rocks, but neither compositional variation nor paragenesis of this mineral has been studied in great detail. Only a few electron-microprobe datasets of miserite are available in the literature (Scott 1976, Lazebnik & Lazebnik 1981). Miserite from Dara-i-Pioz is similar in composition to the material from Kipawa, Quebec, for which the structural formula was derived by Scott (1976). In both cases, the mineral contains appreciable levels of Y (up to 4.4 wt.% Y_2O_3) and a relatively small amount of K in the *Z* site (0.2–0.3 *apfu*). Miserite from perpotassic rocks of the Murun complex, in Siberia, is virtually devoid of Y and comparatively enriched in K (>0.4 *apfu* in the *Z* site) (Lazebnik & Lazebnik 1981, authors' unpubl. data).

In the quartz – albite – aegirine rock, *turkestanite* occurs as apple-green and yellowish prismatic crystals poikilitically enclosing the groundmass minerals (Fig. 2e). Such crystals, termed "metacrysts" in the Russian geological literature, are very common in alkaline metasomatic rocks and typically consist of minerals enriched in Zr, *REE*, Th, Sr and Ti (zircon, loparite, lamprophyllite and astrophyllite, among others). The "metacrysts" are interpreted as products of crystallization from late-stage interstitial fluids (*e.g.*, Sinai & Chakhmouradian 1995).

The composition of turkestanite is broadly similar to that of other double-ring Th silicates, including steacyite and ekanite. In contrast to ekanite, $Ca_2Th[Si_8O_{20}]$, turkestanite contains appreciable K, and corresponds to a Ca-dominant analogue of steacyite (Table 1). A mineral of such composition was first described under the name "Th–Ca–K silicate" by Ginzburg *et al.* (1965). Perrault & Szymański (1982) revised the nomenclature of ekanite-related phases, and suggested that the "Th–Ca–K silicate" probably represents a new mineral species. The new mineral received official recognition as turkestanite after its re-investigation by Pautov *et al.* (1997).

As the idealized structural formula corresponding to the turkestanite end-member, $(K_{1-x}\square_x)Ca_2Th[Si_8O_{20}]$, is not charge-balanced, some substitution of Na for Ca, or *REE* for Th must be invariably present in this mineral. Hence, neither end-member turkestanite nor steacyite is possible, and only intermediate compositions occur in nature. The type material of Pautov *et al.* (1997) and samples examined in the present study (Table 6) contain significant levels of both Na and *REE* (up to 2.9 and 2.6 wt.% oxides, respectively). Turkestanite from the quartz – albite – aegirine rock shows relatively little variation in composition, and is strongly enriched in U and Pb, but depleted in K in comparison with the type material. The ionic radii of U and *REE* (Shannon 1976), and the previously published analytical data on steacyite (Perrault & Szymański 1982, Parodi & Della Ventura 1987) suggest that U enters the Th site, whereas *REE* can be accommodated in both Th and Ca sites in the structure. The Pb^{2+} cations cannot be assigned with the same degree of certainty. As the amount of Pb in our samples of turkestanite exceeds that required to fill the Ca site, some Pb probably enters the partially vacant K site. Regardless of the difference in size between K^+ and Pb^{2+} (Shannon 1976), substitution between these two elements has been documented in a number of minerals (*e.g.*, hyalotekite: Grew *et al.* 1994). In turkestanite, this substitution is facilitated by incomplete occupancy in the K site, and may indicate the existence of a distinct steacyite-group end-member, $Pb_{1/2x}(Ca_{1-x}Na_x)_2Th[Si_8O_{20}]$.

The youngest mineral assemblage in the quartz – albite – aegirine rock includes rare minerals enriched in B, *REE*, Ba and high-field-strength elements (Ti, Zr, Sn and Hf) that are associated with quartz, datolite and fluorite. These minerals fill fractures within the earlier-crystallized phases (aegirine, baratovite, microcline and miserite). The mineralized fractures do not exceed a few hundred micrometers in thickness, and contain euhedral to subhedral crystals of bazirite, stillwellite, tadzhikite, zircon and titanite. In terms of composition, fluorite and datolite are close to their theoretical formulae. Calcite may or may not be a part of this paragenesis (see below). It occurs as both fracture fillings and anhedral grains up to a few mm in size. Where rimmed by calcite, the earlier-formed minerals commonly exhibit resorption textures. Interestingly, the calcite is entirely devoid of lamellar twinning, but shows conspicuous strain-induced features, such as bending of the grains around the feldspars, strong undulatory extinction and curved cleavage. Chemically, this mineral is akin to primary calcite in calcio-carbonatites in containing high levels of Sr (1.1–1.3 wt.% SrO) and negligible Mg, Mn and Fe contents (<0.1 wt.% of the respective oxides).

Tadzhikite is abundant as fibrous aggregates up to 150 μm across that are confined to fractures. Where hosted by miserite, these aggregates are invariably accompanied by areas of *REE* depletion in the host mineral. Some aggregates enclose minute (*ca.* 5 μm) euhedral crystals of low-Ta uranoan pyrochlore (*ca.* 25 wt.% UO_2, ≤1.2 wt.% Ta_2O_5). The lumps of tadzhikite consist of kinked and intertwining fibers showing undulatory extinction in crossed polars. In thin section, the mineral has a pale yellow color, high positive relief, low birefringence and, in contrast to stillwellite, is transparent. In BSE, optically uniform aggregates of tadzhikite appear to consist of two intricately intergrown varieties, enriched respectively in the light *REE* and Y. The bulk of the tadzhikite lumps is composed of the high-atomic-number *LREE*-enriched phase, with up to 31 wt.% $LREE_2O_3$ and 1.3–7.8 wt.% Y_2O_3 (Table 7, anal. 1–3). Darker zones with lower atomic number correspond to tadzhikite with higher Y contents (up to 10.3 wt.% Y_2O_3, Table 7, anal. 4–5). The structure of non-metamict tadzhikite has been refined recently by Hawthorne *et al.* (1998). These authors demonstrated that there is a high degree of order of Si and B in the tetrahedral positions, Al enters the octahedrally coordinated Ti sites rather than the tetrahedra, and the proportion of large cations per formula unit (Ca + *REE*, *apfu*) is variable owing to the incomplete occupancy of the *REE* site. Consequently, the composition of tadzhikite determined by the electron-microprobe method is best recalculated on the basis of four atoms of Si per formula unit (Hawthorne *et al.* 1998). Tadzhikite from the quartz – albite – aegirine rock shows the compositional range described by the empirical formula $Ca_{3.2-3.8}LREE_{1.0-1.8}Y_{0.1-0.9}(Ti,Fe,Al)_{1.0}[B_4Si_4O_{20.3}(OH)_{1.7}](OH)_2$, which is in excellent agreement with the structural formula of the mineral determined by Hawthorne *et al.* (1998).

TABLE 7. REPRESENTATIVE COMPOSITIONS OF TADZHIKITE AND STILLWELLITE FROM THE DARA-I-PIOZ COMPLEX

	TADZHIKITE					STILLWELLITE	
Wt.%	1	2	3	4	5	6	7
CaO	19.95	19.3	20.61	22.51	21.94	0.24	0.29
MgO	0.16	0.21	n.d	n.d	n.d	n.d	n.d
Fe_2O_3	2.61	2.53	3.95	4.20	3.92	n.d	n.d
Al_2O_3	0.85	0.94	0.59	0.48	0.51	0.06	n.d
Y_2O_3	1.34	2.36	5.69	8.64	10.31	n.d	n.d
La_2O_3	2.99	2.83	4.23	1.68	2.18	16.97	16.77
Ce_2O_3	13.63	12.88	11.91	7.12	5.80	35.19	35.54
Pr_2O_3	1.96	1.72	0.85	1.74	1.14	2.11	3.01
Nd_2O_3	9.84	8.96	5.97	7.17	5.75	8.43	7.65
Eu_2O_3	0.24	0.82	n.d	n.d	1.01	n.d	n.d
Gd_2O_3	0.77	1.22	0.35	0.85	1.48	n.d	n.d
Sm_2O_3	1.70	1.42	0.58	0.99	1.73	n.d	n.d
UO_2	0.88	1.02	n.d	n.d	n.d	n.d	n.d
TiO_2	3.76	3.12	2.83	2.92	3.18	n.d	n.d
SiO_2	25.78	25.71	24.17	25.21	25.39	23.13	23.24
B_2O_3*	14.93	14.89	14.00	14.60	14.71	13.40	13.46
Total	101.39	99.93	95.73	98.11	99.05	99.53	99.96
	Structural formulae calculated on the basis of:						
			Si = 4			O = 5	
Ca	3.317	3.217	3.655	3.827	3.704	0.011	0.013
Mg	0.037	0.049	-	-	-	-	-
Fe^{3+}	0.305	0.296	0.492	0.501	0.465	-	-
Al	0.155	0.172	0.115	0.090	0.095	0.003	-
Y	0.111	0.195	0.501	0.730	0.864	-	-
La	0.171	0.162	0.258	0.098	0.127	0.270	0.266
Ce	0.774	0.734	0.722	0.414	0.335	0.557	0.560
Pr	0.111	0.098	0.051	0.101	0.065	0.033	0.047
Nd	0.545	0.498	0.353	0.406	0.324	0.130	0.118
Eu	0.013	0.044	-	-	-	-	-
Gd	0.040	0.063	0.019	0.045	0.077	-	-
Sm	0.091	0.076	0.033	0.054	0.094	-	-
U	0.016	0.018	-	-	-	-	-
Ti	0.439	0.365	0.352	0.348	0.377	-	-
Si	4.000	4.000	4.000	4.000	4.000	0.999	1.000
B	4.000	4.000	4.000	4.000	4.000	1.000	1.000

n.d = not detected. * B_2O_3 calculated on the basis of stoichiometry.

In both varieties of tadzhikite examined in this study, the sum of light lanthanides (*apfu*) is greater than the amount of Y, and *LREE* are dominated by Ce (Ce > Nd > La ≥ Pr > Sm ≥ Gd). However, in the low-atomic-number zones and, locally, in the high-atomic-number areas within tadzhikite, the proportion of Y does exceed that of Ce (Table 7, anal. 4–5). Thus, the composition of this mineral suggests the existence of two closely related mineral species, "tadzhikite-(Ce)" and "tadzhikite-(Y)". Hawthorne *et al.* (1998) argued that Y in the structure of tadzhikite is accommodated at one of the *Ca* sites rather than competing with Ce for the partially vacant *REE* site, and that the name "tadzhikite-(Y)" is not justified from a crystallographic perspective. They

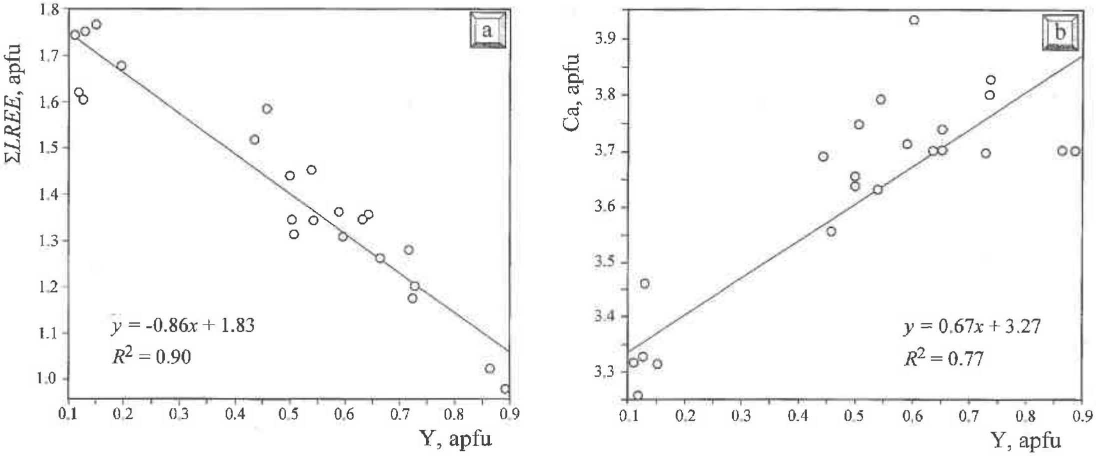

FIG. 3. Correlation diagram of Y *versus* *LREE* (a) and of Y *versus* Ca (b) for tadzhikite from Dara-i-Pioz.

concluded that, although some samples do show the preponderance of Y among *REE* +Y, they should still be termed "tadzhikite-(Ce)". The incorporation of Y in the *Ca* sites, and complete occupancy at these sites, would most probably result in negative correlation between Y and Ca, whereas no correlation should be expected between Y and *LREE*, given that *LREE* enter independent eight-coordinated sites in the structure of tadzhikite (Hawthorne *et al.* 1998). However, our data clearly demonstrate that the concentration of Y in tadzhikite increases with decreasing *LREE*, and shows very little correlation with the Ca content (Fig. 3). Importantly, our samples of tadzhikite contain somewhat higher levels of Ca, compared with the material of Hawthorne *et al.* (1998). Hence, we suggest here that enrichment of tadzhikite in Ca may result in nearly complete occupancy of the *Ca* sites, and "force" Y to enter the *REE* sites normally occupied by Ce and other light lanthanides. Further, the excess Y accommodated in the *REE* sites may exceed the content of any individual light *REE*, thereby justifying the name "tadzhikite-(Y)". One such an example is represented by composition 5 in Table 7, which contains 0.57 *apfu* Y and only 0.34 *apfu* Ce at the *REE* site. Also, it is noteworthy that the *REE*(1) and *REE*(4) polyhedra in the structure of tadzhikite are virtually indistinguishable from the two *Ca* polyhedra in terms of size (Hawthorne *et al.* 1998, Table 3), and thus likely to incorporate Y just as readily as they do *LREE*. Further discussion of this problem is beyond the scope of this work and requires structural studies of compositionally different samples of tadzhikite.

Stillwellite-(Ce) is relatively common as hexagonal crystals lining fractures and cavities; most crystals are smaller than 50 μm, and typically accompany tadzhikite. Stillwellite-Ce from Dara-i-Pioz is relatively "sterile" in composition and approaches the ideal formula *LREE*[$BSiO_5$], where Ce > La > Nd > Pr (Table 7, anal. 6–7). Stillwellite from other occurrences has a very similar composition, but may contain a significant amount of Th substituting for the *LREE* (Burns *et al.* 1993).

Titanite is relatively common in the quartz – albite – aegirine rock, and occurs as two major morphological types: (i) anhedral to subhedral crystals up to 400 μm enclosed in prismatic aegirine (Fig. 2f), and (ii) small wedge-shaped crystals (<100 μm) and their intergrowths filling fractures in baratovite and, less commonly, other earlier-crystallized minerals (Fig. 4). Crystals of type (i) typically have a rounded shape and are not spatially associated with fractures in the aegirine host. This titanite most probably represents remnants of an early paragenesis preserved from resorption by entrapment in aegirine. Titanite of type (ii) is undoubtedly a late-stage mineral, as it is confined to fractures, and invariably associated with datolite, zircon, bazirite or *REE* borosilicates.

The two types of titanite also differ in composition. The relict crystals of type (i) are devoid of zonation and show very little intergranular variation in composition, approaching the ideal formula $CaTiSiO_5$ (Table 8, anal. 1). Al, *REE* and Sn were sought but not found in this titanite, whereas Zr and Nb are present only in trace amounts. Titanite of type (ii) is invariably enriched in minor elements, predominantly in Nb (Table 8, anal. 2). The compositionally most unusual titanite occurs in an assemblage with zircon and datolite, where it forms intricately zoned euhedral crystals with a darker, low-atomic-number core, and an oscillatory brighter rim (Fig. 4). The difference in atomic number is created by higher Sn, Zr and Nb contents in the rim relative to the core. The enrichment in heavy elements is accompanied by a decrease in Al and Fe from the core outward (Fig. 5). The outermost zones of the crystals contain up to 8.1 wt.% SnO_2, 2.3% ZrO_2 and 1.7% Nb_2O_5

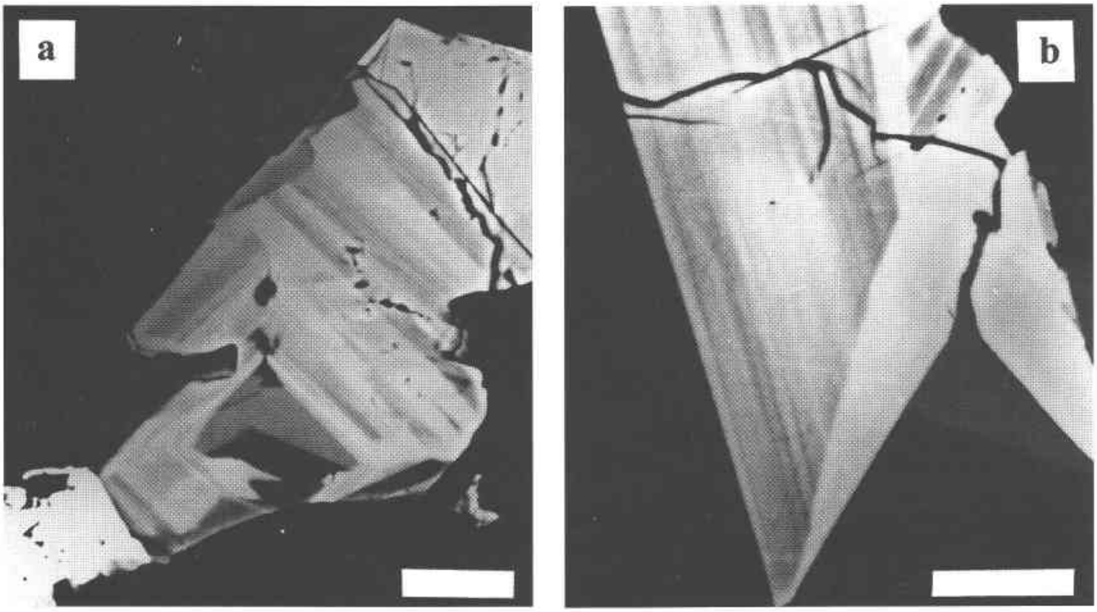

FIG. 4. Zonation of titanite crystals filling fractures in the quartz – albite – aegirine rock, Dara-i-Pioz complex. Back-scattered electron images. Scale bar is 20 μm for both images. (a) Crystal zoned from an Al–Fe-enriched core (dark) through an oscillatory intermediate zone to a Sn–Zr-enriched rim (bright). (b) Oscillatorily zoned euhedral crystal.

(Table 8, anal. 3–5). This combination of elements, at their relatively high concentrations, is unparalleled by any naturally occurring titanite. Enrichment in Sn is characteristic of titanite from Sn-bearing skarns, and may culminate in the appearance of malayaite, $CaSnSiO_5$, in relatively high-temperature assemblages (*e.g.*, Chen *et al.* 1992). Simultaneous substitution of Ti by Sn and Nb (up to 7.4 and 6.2 wt.% oxides, respectively) has been observed in titanite from granitic pegmatites of Żólkiewka, Poland (Janeczek 1996). Significantly lower Sn and higher Nb contents have been detected in titanite from calc-silicate metamorphic rocks of Gebel Umm Shagir, Egypt (Bernau & Franz 1987). Finally, coupled enrichment in Nb and Zr (≤1.5 wt.% Nb_2O_5 and 4.2% ZrO_2) is observed in titanite from xenoliths of nepheline syenite at Oldoinyo Lengai, Tanzania (Dawson *et al.* 1995). Importantly, the material from Oldoinyo Lengai, as well as Nb- or Zr-enriched titanite from other occurrences of nepheline syenite, lack any appreciable Sn contents (*e.g.*, Woolley *et al.* 1992, Chakhmouradian & Mitchell 1999). Figure 6 illustrates the overall evolutionary trend of zoned titanite (ii) from Dara-i-Pioz expressed in terms of three major end-member components: titanite (Tit), malayaite (Mal) and $CaZrSiO_5$. This diagram shows that mineral compositions between approximately $Tit_{86}Mal_{14}$ and $Tit_{12}Mal_{88}$ are apparently very rare in nature, although the complete solid-solution series $CaTi_{1-x}Sn_xSiO_5$ has been synthesized (Kunz *et al.* 1997).

TABLE 8. REPRESENTATIVE COMPOSITIONS OF TITANITE, BAZIRITE AND ZIRCON FROM THE DARA-I-PIOZ COMPLEX

	TITANITE					BAZIRITE	ZIRCON
Wt.%	1	2	3	4	5	6	7
Na_2O	0.40	0.31	n.d	n.d	n.d	0.53	n.a
K_2O	n.d	n.d	n.d	n.d	n.d	0.20	n.a
CaO	28.02	27.57	28.28	27.84	27.31	0.76	0.31
BaO	n.a	n.a	n.a	n.a	n.a	30.68	n.a
Ce_2O_3	n.d	0.46	0.42	0.30	0.10	n.a	n.a
Al_2O_3	n.d	n.d	1.37	0.66	0.10	0.25	n.a
Fe_2O_3*	1.27	0.95	2.43	2.40	1.98	0.14	n.d
TiO_2	39.26	38.62	35.24	35.15	31.20	n.d	0.09
ZrO_2	n.d	n.d	0.20	0.27	2.31	22.68	63.93
SnO_2	n.d	0.23	0.64	3.67	8.13	2.93	n.d
HfO_2	n.a	n.a	n.a	n.a	n.a	2.10	3.19
Nb_2O_5	0.18	1.51	0.15	0.48	1.60	n.a	0.29
SiO_2	30.81	30.47	29.27	29.05	29.00	39.38	31.77
Total	99.94	100.12	98.00	99.82	101.73	99.65	99.58
Structural formulae calculated on the basis of:							
	$\sum$cations = 3					O = 9	O = 4
Na	0.025	0.020	-	-	-	0.078	-
K	-	-	-	-	-	0.019	-
Ca	0.976	0.971	1.009	0.996	0.992	0.062	0.010
Ba	-	-	-	-	-	0.913	-
Ce	-	0.006	0.005	0.004	0.001	-	-
Al	-	-	0.054	0.026	0.004	0.022	-
Fe*	0.031	0.023	0.061	0.060	0.050	0.008	-
Ti	0.960	0.954	0.882	0.883	0.796	-	0.002
Zr	-	-	0.003	0.004	0.038	0.840	0.968
Sn	-	-	0.008	0.049	0.110	0.089	-
Hf	-	-	-	-	-	0.046	0.028
Nb	0.003	0.022	0.002	0.007	0.024	-	0.004
Si	1.002	1.001	0.975	0.970	0.983	2.991	0.987

* Total Fe given as Fe_2O_3. n.a = not analyzed; n.d = not detected.

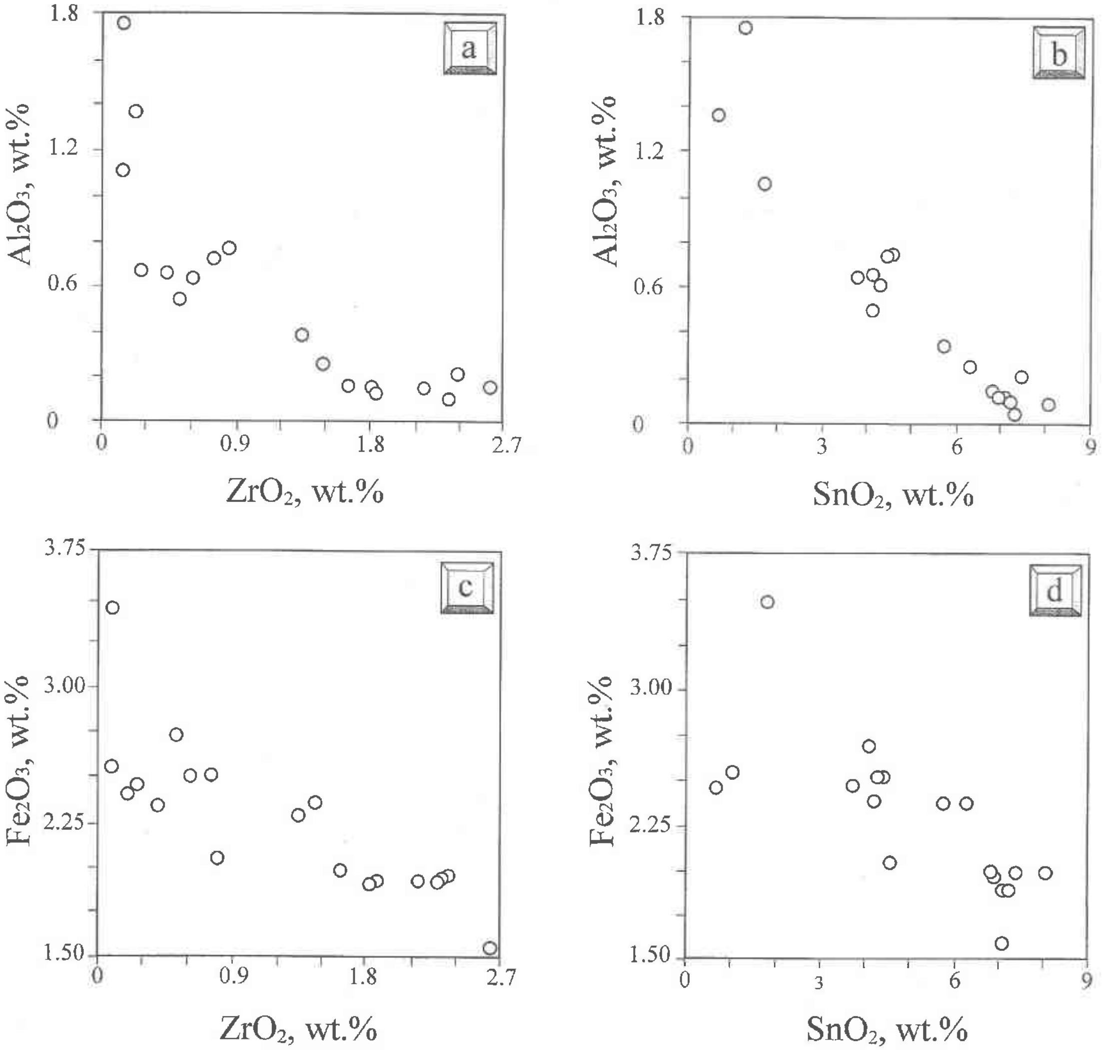

FIG. 5. Variation in minor components in the composition of late-generation titanite from Dara-i-Pioz.

Bazirite occurs in an assemblage with titanite as fracture fillings in baratovite and aegirine. This mineral was not observed in association with zircon. Discrete crystals of bazirite are rare and do not exceed a few tens of µm across. Previously, bazirite has been observed as a minor constituent of alkali granites on Rockall Island, Scotland (Young *et al.* 1978), in Ba-rich contact-metamorphic rocks at Big Creek, California (Alfors & Pabst 1984), and in pseudomorphs after eudialyte at Dara-i-Pioz (Pautov & Khvorov 1998). Bazirite from the quartz – albite – aegirine rock is unusual in having high Sn (Table 8, anal. 6), similar to "evolved" titanite associated with zircon. Also, all compositions of bazirite obtained in the present work are enriched in alkalis, and show an excess of large cations (ΣBa + Na + K + Ca) per formula unit. These chemical characteristics delineate a trend toward pabstite, $BaSn[Si_3O_9]$, and structurally related zirconosilicates with the general formula $(K,Na)_2Zr[Si_3O_9]$. In the absence of bazirite, Zr is concentrated predominantly in *zircon* and, to a lesser degree, in titanite (see above). Zircon from Dara-i-Pioz is noticeably enriched in Hf (Table 8, anal. 7).

DISCUSSION

The albite-bearing rocks of the Dara-i-Pioz complex are generally interpreted as products of metasomatic alteration (albitization) of the syenitic suite (Dusmatov

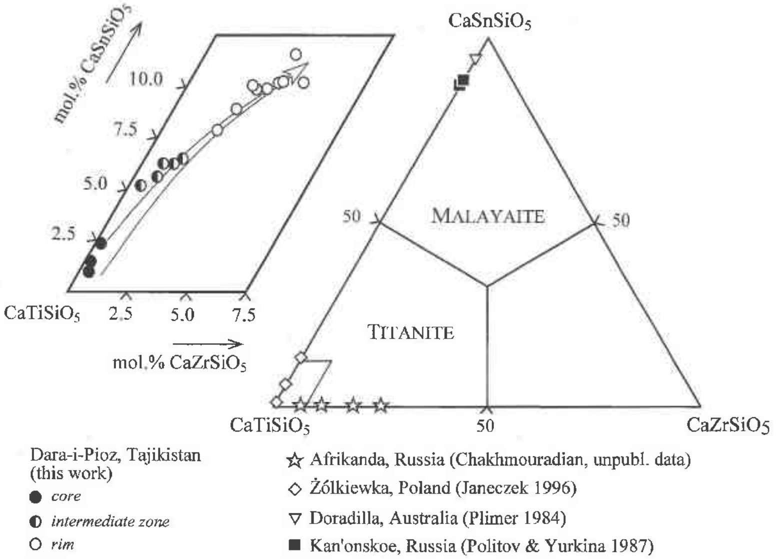

FIG. 6. Compositions (mol.%) of Sn–Zr-enriched titanite from Dara-i-Pioz in the system $CaTiSiO_5$ – $CaSnSiO_5$ – $CaZrSiO_5$. Arrow indicates a core-to-rim zonation trend (see Fig. 4a for a typical pattern of zonation). Also shown are some Zr- and Sn-enriched compositions from carbonatites, granitic pegmatites and skarns.

et al. 1973). During metasomatism, primary textural features of the igneous rocks may be partially preserved as relict mineral fragments and inherited grain orientations (Krasnova 1988). In the quartz – albite – aegirine rock, such a relict assemblage may include anhedral grains of aegirine and titanite enclosed by prismatic aegirine. As demonstrated in the previous section, these minerals differ in composition from their counterparts in the later-crystallized assemblage. It is unclear whether the grains of microcline hosted by prismatic aegirine belong to the relict paragenesis, as these inclusions are compositionally indistinguishable from the large crystals associated with albite. Both varieties of microcline could crystallize at the final stages of aegirine precipitation nearly simultaneously with albite, which also occurs as a groundmass phase and inclusions in aegirine.

The petrography and mineralogy of the quartz – albite – aegirine rock provide very few clues to the paragenesis from which the relict aegirine and titanite originate. The noticeable difference in Mg content between the relict and prismatic aegirine (Fig. 1) may be interpreted as a result of: (i) different $f(O_2)$ during the crystallization of the two types of clinopyroxene, (ii) competition for Fe^{2+} between aegirine and other, as yet unknown mafic minerals in the relict paragenesis, or (iii) generally lower levels of Mg in the metasomatic system (*cf.* data of Woolley & Platt 1986, Mitchell & Vladykin 1996, Piilonen *et al.* 1998). As the compositions of relict and prismatic aegirine define two independent trends in the diagram $NaFe^{3+}Si_2O_6$ – $CaFe^{2+}Si_2O_6$ – $CaMgSi_2O_6$, we can conclude that an alkali-rich metasomatic fluid was derived from an external source, rather than fractionated from a magma that precipitated the relict paragenesis. In other words, the quartz – albite – aegirine rock does not represent a product of postmagmatic closed-system re-equilibration of an alkaline syenitic parent. This conclusion is further supported by the noticeable difference in concentrations of minor elements in the relict and metasomatic titanite. Among these elements, Nb and Ce are of particular relevance to our case, as they are effectively sequestered from a melt (or fluid) by titanite owing to the high capacity of its structure to incorporate these elements (Russell *et al.* 1994, Černý *et al.* 1995). The low levels of Nb and Ce in the relict titanite suggest that it crystallized from a primitive, unevolved magma.

The most prominent textural feature that bears on conditions of crystallization of the quartz – albite – aegirine rock is the evidence of syndeformational growth recorded in a mosaic of quartz grains (Fig. 2a). This feature clearly indicates at least two episodes of growth of quartz. The bulk of the quartz precipitated after the feldspars, aegirine and baratovite, probably forming a uniform mosaic of more-or-less equant grains. Subsequently, the quartz – albite – aegirine rock underwent deformation, resulting in nucleation of the smaller crystals of quartz at the grain boundaries owing to some inhomogeneity in intragranular stress (Hickey & Bell 1996). As increasing temperature would decrease the rate of nucleation of quartz grains (N), and increase the rate at which the grains are consumed by grain-boundary migration (*G*), the observed syndeformational texture indicates that the ratio *N/G* was maintained at the same level or increased during the deformation (for example, owing to increasing strain-rate), and that the rock has not undergone post-tectonic annealing (Hickey & Bell 1996). On the other hand, the rate of recrystallization is positively correlated with fluid content, and the textural effect of annealing may be retarded in a fluid-rich metasomatic environment. Undoubtedly, during the deformation event, some silica was remobilized by a fluid, and redeposited as quartz filling fractures within the earlier-crystallized phases (aegirine, microcline, baratovite and miserite).

The association of late quartz with datolite, fluorite, rare-earth borosilicates, Sn–Zr–Nb-bearing titanite, Sn–Hf-bearing bazirite and Hf-bearing zircon suggests that the fluid circulating in the system during the deformation event was enriched in B, F and incompatible elements (*REE*, Ba, Zr, Sn, Hf and Nb). It may have represented an evolved portion of the primary fluid involved in albitization (*sensu* Dusmatov *et al.* 1973) or, alternatively, fractionated from an independent source. One such source could be alkaline pegmatites that intrude the metasomatic rocks, and are characterized by elevated B contents (Grew *et al.* 1993). On the average, the pegmatites contain 415 ppm B, as opposed to 60 ppm in the albitites (Dusmatov *et al.* 1973). In common with the quartz – albite – aegirine rock, the pegmatites host a similar assemblage of rare minerals, including stillwellite-(Ce), tadzhikite and Zr-bearing phases. A more detailed account of the mineralogy and geochemistry of the pegmatites is given by Belakowski (1991) and Grew *et al.* (1993).

The presence of datolite in the fracture-filling paragenesis suggests crystallization temperatures in the range 300–500°C, whereas the successive precipitation of quartz, datolite (not danburite) and fluorite is indicative of progressively increasing alkalinity, and decreasing $a(SiO_2)$ and temperature (Lisitsyn & Malinko 1971). It is noteworthy that danburite does occur at Dara-i-Pioz, but, in contrast to datolite, it must be confined to higher-temperature assemblages (Grew *et al.* 1993, Grew 1996). The nearly contemporaneous crystallization of titanite, zircon and bazirite with datolite and other borosilicates may indicate that high-field-strength elements such as Ti, Zr, Hf, Sn and Nb were initially present in the fluid as borate complexes. The experimental and mineralogical data on rare-element pegmatites provide further evidence for complexation of Group-IV and Group-V elements with B (London 1987). From the data of Aja *et al.* (1995) on the complexation of Zr in hydrothermal systems, we infer that high Ca contents in the B–F-rich fluid at Dara-i-Pioz probably precluded bonding of the high-field-strength elements with F. Gradual dissociation of the borate complexes throughout the crystallization span of titanite probably accounts for the observed core-to-rim zonation pattern of this mineral (Fig. 5). Note also that titanite in the fracture-filling assemblage is characteristically depleted in Al, and only cores of some crystals contain up to 1.8 wt.% Al_2O_3. It is well known that incorporation of Al in this mineral is promoted by high activities of F (Enami *et al.* 1993, Carswell *et al.* 1996), and that aluminian titanite $Ca(Ti,Al)SiO_4(O,F)$ in relatively high-pressure assemblages is commonly accompanied by fluorite (Franz & Spear 1985). On the other hand, hydrothermal titanite that precipitates under low pressures and temperatures also may incorporate significant amounts of Al, predominantly as the component $CaAlSiO_4(OH)$ (Enami *et al.* 1993). Thus, the compositional features of the Dara-i-Pioz titanite indicate that the late-stage B–F-rich fluid was severely depleted in Al.

It is uncertain whether crystallization of Sr-enriched calcite in the quartz – albite – aegirine rock is related to the hydrothermal event involving the B–F-rich fluid, or resulted from interaction of the rock with a carbothermal fluid. The mineralized fractures are characteristically devoid of Sr minerals, and even the silicates concentrating large-ion lithophile elements [stillwellite-(Ce), titanite, tadzhikite and bazirite] lack detectable Sr. The conspicuous strain-induced features observed in the Sr-enriched calcite from the quartz – albite – aegirine rock may suggest that this mineral formed prior to the major deformation event, *i.e.*, somewhat earlier than the borosilicates and associated Zr–Sn-bearing phases. On a larger scale, carbonate rocks of the Dara-i-Pioz complex postdate the albite-bearing assemblages, and, according to Dusmatov *et al.* (1973), manifest an independent metasomatic event, *i.e.*, carbonatization. Unfortunately, we were unable to find any data on the composition of calcite from the carbonate and quartz–carbonate units, and thus cannot comment on its compositional similarity to the Sr-enriched calcite from the quartz – albite – aegirine rock. The observed relationships between the major and accessory minerals from Dara-i-Pioz, and an inferred order of their crystallization, are summarized in a paragenetic bar diagram (Fig. 7).

CONCLUSIONS

The quartz – albite – aegirine rock represents a product of multistage alkali metasomatism of an igneous precursor involving fluids derived from two or three different sources. The primary mineral assemblage was developed during the albitization of an alkaline syenitic parent. This assemblage is composed of albite, microcline, aegirine – hedenbergitic clinopyroxene, baratovite, miserite, fluorapatite, quartz and turkestanite. Sr-enriched calcite is present in relatively minor quantities and probably crystallized during a later metasomatic event (carbonatization ?). The crystallization of the quartz – albite – aegirine rock was followed by

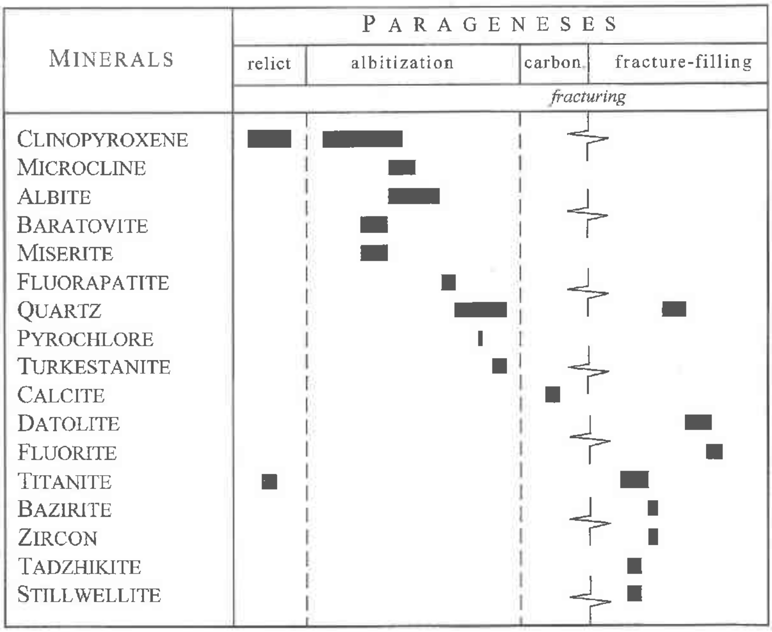

FIG. 7. A simplified paragenetic diagram for the quartz – albite – aegirine rock, Dara-i-Pioz complex. Note the occurrence of some minerals in more than one paragenesis. For further discussion, see text.

deformation and fracturing, and precipitation of quartz, datolite and fluorite in the fractures. The fractures also host titanite, tadzhikite, stillwellite-(Ce), bazirite and zircon. This late assemblage of minerals is believed to have crystallized from a fluid enriched in B, F, *REE*, Ba and high-field-strength elements (Ti, Zr, Nb, Sn and Hf), and depleted in Al. Presumably, this fluid was fractionated from B-rich alkaline pegmatites cross-cutting the metasomatic rocks.

ACKNOWLEDGEMENTS

We are very grateful to Roger H. Mitchell and Allan MacKenzie whose generous offer to use the instrumental facility at Lakehead University (Ontario) made our study possible. We also thank Robert F. Martin, Edward S. Grew and Alexander U. Falster for their constructive comments on the early version of the manuscript.

REFERENCES

AJA, S.U., WOOD, S.A. & WILLIAMS-JONES, A.E. (1995): The aqueous geochemistry of Zr and the solubility of some Zr-bearing minerals. *Appl. Geochem.* **10**, 603-620.

ALFORS, J.T. & PABST, A. (1984): Titanian taramellites in western North America. *Am. Mineral.* **69**, 358-373.

BELAKOWSKI, D.I. (1991): Die seltenen Mineralien von Dara-i-Pioz im Hochgebirge Tadshikistans. *Lapis* **16**(12), 42-48.

BERNAU, R. & FRANZ, G. (1987): Crystal chemistry and genesis of Nb-, V-, and Al-rich metamorphic titanite from Egypt and Greece. *Can. Mineral.* **25**, 695-705.

BURNS, P.C., HAWTHORNE, F.C., MACDONALD, D.J., DELLA VENTURA, G. & PARODI, G.C. (1993): The crystal structure of stillwellite. *Can. Mineral.* **31**, 147-152.

CARSWELL, D.A., WILSON, R.N. & ZHAI, M. (1996): Ultra-high pressure aluminous titanites in carbonate-bearing eclogites at Shuanghe in Dabieshan, central China. *Mineral. Mag.* **60**, 461-471.

ČERNÝ, P., NOVÁK, M. & CHAPMAN, R. (1995): The Al(Nb,Ta)Ti_{-2} substitution in titanite: the emergence of a new species? *Mineral. Petrol.* **52**, 61-73.

CHAKHMOURADIAN, A.R. & MITCHELL, R.H. (1999): Primary, agpaitic and deuteric stages in the evolution of accessory Sr, REE, Ba and Nb-mineralization in nepheline-syenite pegmatites at Pegmatite Peak, Bearpaw Mts., Montana. *Mineral. Petrol.* (in press).

CHEN, J., HALLS, C. & STANLEY, C.J. (1992): Tin bearing skarns of South China: geological setting and mineralogy. *Ore Geol. Rev.* **7**, 225-248.

Dawson, J.B., Smith, J.V. & Steele, I.M. (1995): Petrology and mineral chemistry of plutonic igneous xenoliths from the carbonatite volcano, Oldoino Lengai, Tanzania. *J. Petrol.* **36**, 797-826.

Dusmatov, V.D., Mogarovskiy, V.V. & Koreshina, Yu.B. (1973): Boron geochemistry in the granite–syenite intrusions in the R. Darai Piyez, south Tien Shan. *Geochem. Int.* **10**(9), 871-875.

________, Semenov, E.I., Khomyakov, A.P, Bykova, A.V. & Dzhafarov, N.K. (1975): Baratovite, a new mineral. *Zap. Vses. Mineral. Obshchest.* **104**, 580-582 (in Russ.).

Enami, M., Suzuki, SK, Liou, J.G. & Bird, D.K. (1993): Al–Fe^{3+} and F–OH substitutions in titanite and constraints on their P–T dependence. *Eur. J. Mineral.* **5**, 219-231.

Fleischer, M. (1987): *Glossary of Mineral Species.* Mineralogical Record Inc., Tucson, Arizona.

Franz, G. & Spear, F.S. (1985): Aluminous titanite (sphene) from the eclogite zone, south-central Tauern Window, Austria. *Chem. Geol.* **50**, 33-46.

Ginzburg, I.V, Semenov, E.I., Leonova, L.L., Sidorenko, G.A. & Dusmatov, V.D. (1965): Alkali-rich crystalline ekanite from the central Asia. *Tr. Mineral. Muz. Akad. Nauk SSSR* **16**, 57-72 (in Russ.).

Grew, E.S. (1996): Borosilicates (exclusive of tourmaline) and boron in rock-forming minerals in metamorphic environments. *In* Boron: Mineralogy, Petrology and Geochemistry (E.S. Grew & L.M. Anovitz, eds.). *Rev. Mineral.* **33**, 387-502.

________, Belakovskiy, D.I., Fleet, M.E., Yates, M.G., McGee, J.J. & Marquez, N. (1993): Reedmergnerite and associated minerals from peralkaline pegmatite, Dara-i-Pioz, southern Tien Shan, Tajikistan. *Eur. J. Mineral.* **5**, 971-984.

________, Yates, M.G., Belakovskiy, D.I., Rouse, R.C., Su, Shu-Chun & Marquez, N. (1994): Hyalotekite from reedmergnerite-bearing peralkaline pegmatite, Dara-i-Pioz, Tajikistan and from Mn skarn, Långban, Värmland, Sweden: a new look at an old mineral. *Mineral. Mag.* **58**, 285-297.

Hawthorne, F.C., Cooper, M.A. & Taylor, M.C. (1998): Refinement of the crystal structure of tadzhikite. *Can. Mineral.* **36**, 817-822.

Hickey, K.A. & Bell, T.H. (1996): Syn-deformational grain growth: matrix coarsening during foliation development and regional metamorphism rather than by static annealing. *Eur. J. Mineral.* **8**, 1351-1373.

Janeczek, J. (1996): Nb-, Ta- and Sn-rich titanite and its alteration in pegmatites from Żólkiewka, Poland. *Neues Jahrb. Mineral., Monatsh.*, 459-469.

Korobeinikov, A.N. & Laajoki, K. (1994): Petrological aspects of the evolution of clinopyroxene composition in the intrusive rocks of the Lovozero alkaline massif. *Geochem. Int.* **31**(3), 69-76.

Krasnova, N.I. (1988): Some characteristics and indicators of metasomatic formations. *Zap. Vses. Mineral. Obshchest.* **117**, 545-560 (in Russ.).

Kunz, M., Xirouchakis, D., Wang, Y. & Parise, J.B. (1997): Structural investigations along the join $CaTiOSiO_4$ – $CaSnOSiO_4$. *Schweiz. Mineral. Petrogr. Mitt.* **77**, 1-11.

Lazebnik, K.A. & Lazebnik, Yu.D. (1981): Rare silicates, miserite, canasite and fedorite in charoitic rocks. *In* Mineralogy and Geochemistry of Ultramafic and Mafic Rocks of Yakutia. Yakutsk Branch Acad. Sci. USSR, Yakutsk, Russia, 32-50 (in Russ.).

Lisitsyn, A.Ye. & Malinko, S.V. (1971): Physicochemical conditions for development of borosilicates and borates in limy skarn formation. *Int. Geol. Rev.* **13**, 1773-1780.

London, D. (1987): Internal differentiation of rare-element pegmatites: effects of boron, phosphorus, and fluorine. *Geochim. Cosmochim. Acta* **51**, 403-420.

Menchetti, S. & Sabelli, C. (1979): The crystal structure of baratovite. *Am. Mineral.* **64**, 383-389.

Mitchell, R.H. & Vladykin, N.V. (1996): Compositional variation of pyroxene and mica from the Little Murun ultrapotassic complex, Aldan Shield, Russia. *Mineral. Mag.* **60**, 907-925.

Murakami, N., Kato, T. & Hirowatari, F. (1983): Katayamalite, a new Ca–Li–Ti silicate mineral from Iwagi Islet, southwest Japan. *Mineral. J.* **11**(6), 261-268.

Parodi, G.C. & Della Ventura, G. (1987): Steacyite from the Rouma Isle (Los Islands, Republic of Guinea). *Neues Jahrb. Mineral., Monatsh.*, 233-239.

Pautov, L.A., Agakhanov, A., Sokolova, E.V. & Kabalov, Yu.K. (1997): Turkestanite $Th(Ca,Na)_2(K_{1-x}\square_x)\ Si_8O_{20}\bullet nH_2O$ – a new mineral. *Zap. Vser. Mineral. Obshchest.* **126**(6), 45-55 (in Russ.).

________ & Khvorov, P.V. (1998): Bazirite from Tajikistan. *Zap. Vser. Mineral. Obshchest.* **127**(1), 80-83 (in Russ.).

Pekov, I.V., Chukanov, N.V., Eletskaya, O.V., Khomyakov, A.P. & Men'shikov, Yu.P. (1995): Belovite-(Ce): new data, refined formula, and relationships to other minerals of the apatite group. *Zap. Vser. Mineral. Obshchest.* **124**(2), 98-110 (in Russ.).

Perrault, G. & Szymański, J.T. (1982): Steacyite, a new name, and a re-evaluation of the nomenclature of "ekanite"-group minerals. *Can. Mineral.* **20**, 59-63.

Piilonen, P.C., McDonald, A.M. & Lalonde, A.E. (1998): The crystal chemistry of aegirine from Mont Saint-Hilaire, Quebec. *Can. Mineral.* **36**, 779-791.

PLIMER, I.R. (1984): Malayaite and tin-bearing silicates from a skarn at Doradilla via Bourke, New South Wales. *Aust. J. Earth Sci.* **31**, 147-153.

POLITOV, V.K. & YURKINA, K.V. (1987): Titanium malayaite from the Kan'onskoye stanniferous skarn deposit. *Dokl. Acad. Sci. USSR, Earth Sci. Sect.* **300**, 120-122.

RUSSELL, J.K., GROAT, L.A. & HALLERAN, A.A.D. (1994): *LREE*-rich niobian titanite from Mount Bisson, British Columbia: chemistry and exchange mechanisms. *Can. Mineral.* **32**, 575-587.

SANDOMIRSKII, P.A., SIMONOV, M.A. & BELOV, N.V. (1976): The crystal structure of baratovite, $KLi_3Ca_7Ti_2(Si_6O_{18})_2F_2$. *Dokl. Akad. Nauk SSSR* **231**, 615-618 (in Russ.).

SCOTT, J.D. (1976): Crystal structure of miserite, a Zoltai type 5 structure. *Can. Mineral.* **14**, 515- 528.

SHANNON, R.D. (1976): Revised effective ionic radii and systematic studies of interatomic distances in halides and chalcogenides. *Acta Crystallogr.* **A32**, 751-767.

SINAI, M.YU. & CHAKHMOURADIAN, A.R. (1995): An example of comparison between natural and synthetic products of crystal replacement. *Zap. Vser. Mineral. Obshchest.* **124**(5), 47-57 (in Russ.).

WOOLLEY, A.R. & PLATT, R.G. (1986): The mineralogy of nepheline syenite complexes from the northern part of the Chilwa Province, Malawi. *Mineral. Mag.* **50**, 597-610.

________, ________ & EBY, N. (1992): Niobian titanite and eudialyte from the Ilomba nepheline syenite complex, north Malawi. *Mineral. Mag.* **56**, 428-430.

YOUNG, B.R., HAWKES, J.R., MERRIMAN, R.J. & STYLES, M.T. (1978): Bazirite, $BaZrSi_3O_9$, a new mineral from Rockall Island, Inverness-shire, Scotland. *Mineral. Mag.* **42**, 35-40.

Received July 19, 1999, revised manuscript accepted October 19, 1999.